First optical observation of the Moon's sodium exosphere from the lunar orbiter SELENE (Kaguya)

M. Kagitani[1], M. Taguchi[2], A. Yamazaki[3], I. Yoshikawa[4], G. Murakami[4], K. Yoshioka[4], S. Kameda[3], F. Ezawa[4], T. Toyota[4], and S. Okano[1]

[1]*Planetary Plasma and Atmospheric Research Center, Tohoku University, Aramaki-aza-aoba, Aoba, Sendai 980-8578, Japan*
[2]*Rikkyo University, 3-34-1 Nishi-Ikebukuro, Toshima, Tokyo 171-8501, Japan*
[3]*Institute of Space and Astronautical Science, Japan Aerospace Exploration Agency, 3-1-1 Yoshinodai, Sagamihara, Kanagawa 229-8510, Japan*
[4]*Department of Earth and Planetary Science, The University of Tokyo, 7-3-1 Hongo, Bunkyo, Tokyo 113-0033, Japan*

(Received March 16, 2009; Revised April 28, 2009; Accepted April 30, 2009; Online published October 19, 2009)

The first successful observations of resonant scattering emission from the lunar sodium exosphere were made from the lunar orbiter SELENE (Kaguya) using TVIS instruments during the period 17–19 December, 2008. The emission intensity of the NaD-line decreased by 12±6%, with an average value of 5.4 kR (kilorayleighs) in this period, which was preceded, by 1 day, by enhancement of the solar proton flux associated with a corotating interaction region. The results suggest that solar wind particles foster the diffusion of sodium atoms or ions in the lunar regolith up to the surface and that the time scale of the diffusion is a few tens of hours. The declining activity of the Geminid meteor shower is also one possible explanation for the decreasing sodium exosphere.
Key words: Lunar sodium exosphere, lunar orbiter SELENE, resonant scattering emission, Geminid meteor shower.

1. Introduction

In-situ measurements carried out during the Apollo missions revealed that the Moon has a surface boundary exosphere (Hoffman *et al*., 1973; Hodges, 1973, 1975). A major breakthrough in the study of this exosphere occurred with the discovery of D-line emissions of sodium (Na) and potassium (K) from the ground (Potter and Morgan, 1988; Tyler *et al*., 1988). Optical remote sensing techniques enable us to investigate the source mechanism of Na atoms in terms of: (1) thermal desorption, (2) micrometeoroid impacts, (3) photodesorption by solar illumination, and (4) sputtering by solar-wind particles, including chemical reactions (see the review by Stern, 1999). These source mechanisms, which give a wide variety of release velocities and ejection rates acting in different surface regions, produce the characteristic distribution and dynamics of the lunar exosphere. In particular, source mechanisms associated with the solar wind are suppressed for a few days before and after the full moon because the lunar surface is shielded from the solar wind plasma by the Earth's magnetosphere (Potter and Morgan, 1991). Several observational studies have been carried out to test this effect (Potter and Morgan, 1994; Mendillo *et al*., 1999; Potter *et al*., 2000; Wilson *et al*., 2006), although continuous observation from the ground is difficult due to the strong reflection of sunlight during the full moon period.

In this paper, we present the first results of measuring the resonant scattering of Na exosphere ($\lambda_{D2} = 589.0$ nm and $\lambda_{D1} = 589.6$ nm) from the lunar polar orbiter, SELENE (Kaguya). Observations made from the lunar orbit are optimal for continuous observation of Na exosphere.

2. Observations

Observations were made from 16 to 24 December, 2008, using the TVIS (telescope for visible light), which comprises a UPI (upper atmosphere and plasma imager) (Yoshikawa *et al*., 2008) onboard SELENE (Kaguya) (Kato *et al*., 2008). The lunar phase angle (full moon is 0°, and third quarter is 90°) during the observation period changed from 57° through to 147°, thereby spanning the period from the full moon to the new moon. The UPI consists of two imagers, the TVIS and TEX (telescope for extreme-ultraviolet) (Yoshikawa *et al*., 1997, 2002; Yamazaki *et al*., 2002), and a gimbal mount that enables the imagers to be pointed in the desired direction. The TVIS was designed to measure visible light from the Earth's upper atmosphere, such as the aurora and airglow (Taguchi *et al*., 2009). It has a 136-mm clear aperture and a field-of-view of 2.4°. A filter turret with five narrow-band interference filters and a shutter enables changes in observation wavelengths. For our observation, the turret positions of NaD = 589.3 nm, OI = 630.0 nm, and the shutter were used to detect the NaD-line emission and the background continuum and to determine the dark noise levels of a CCD sensor. Details on the specifications of the TVIS are summarized in Table 1 and also given in Taguchi *et al*. (2009).

SELENE is a three-axial stabilized polar orbiter, with one of the axes of the spacecraft always oriented towards the Moon's surface. During the observations, the altitude

Table 1. Specification of UPI-TVIS.

Telescope	$D = 136$ mm, $f = 320$ mm, $F = 2.35$
Filters	Na: λ_c*1 $= 589.6$ nm, λ_{FWHM}*2 $= 2.7$ nm
	OI: $\lambda_c = 630.2$ nm, $\lambda_{FWHM} = 2.0$ nm
Detector	CCD with Peltier cooler (Temp. $= -40$°C)
	Active area: 13.3×13.3 mm, 512×512 pixels
Field-of-view	2.38×2.38°
Pixel scale	0.0047° pixel^{-1}
Sensitivity	40 counts pixel^{-1} s^{-1} Rayleigh^{-1} for 589 nm
	43 counts pixel^{-1} s^{-1} Rayleigh^{-1} for 630 nm

*1Center wavelength of filter transmission.
*2Full-width-half-maximum of filter transmission.

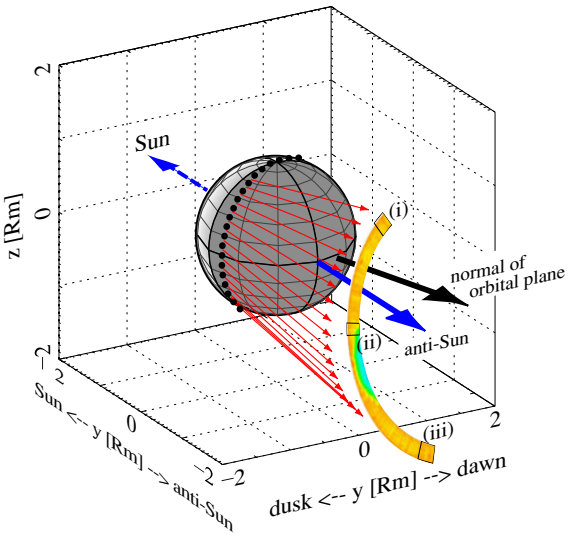

Fig. 1. Spacecraft orbit and field-of-view in the Moon-centered, solar ecliptic (MSE) coordinates on December 17, 2008. Black dotted line shows the spacecraft orbit, and black and blue arrows indicate the normal of the orbital plane and the anti-sunward direction, respectively. Red arrows are field-of-view directions at spacecraft positions during 14:01–14:44 (UT). (i–iii) Field-of-view of spacecraft positions at 14:01, 14:19 and 14:41 (UT), respectively.

Table 2. Observation parameters.

Date (2008)	Time (UT)	Lunar phase*1	Gimbal angles (Az/El)
Dec. 17	14:01–14:44	67°	−248°/72°
Dec. 18	7:37– 8:21	76°	−248°/72°
Dec. 19	1:13– 1:56	85°	−248°/74°
Dec. 19	20:47–21:29	95°	−248°/74°

*1The phase angle of full moon and third quarter correspond to 0° and 90°, respectively.

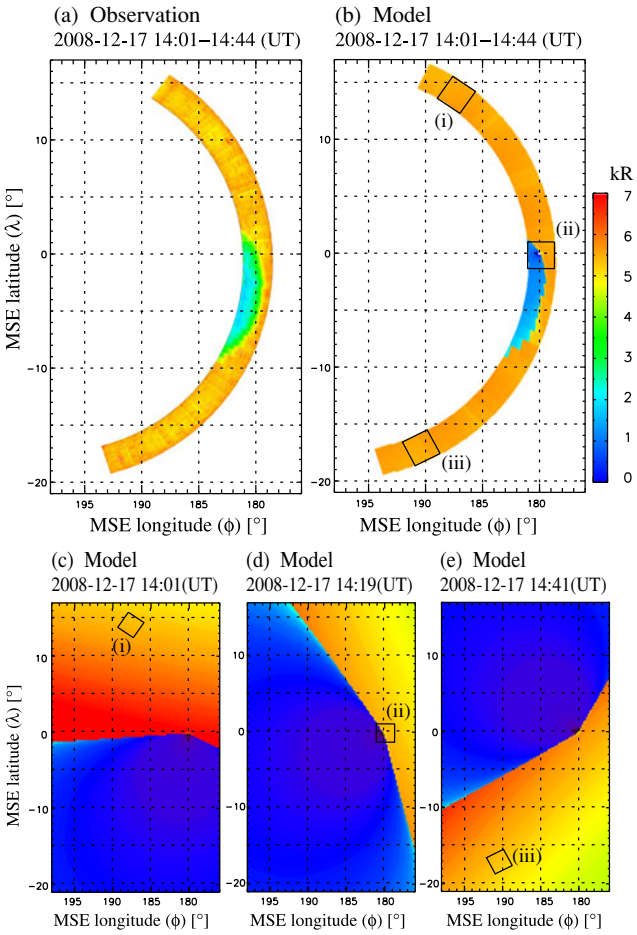

Fig. 2. (a): Distribution of Na emission in MSE coordinates, produced by combining 39 frames, with overlaps at the edge of each frame, acquired during 14:01–14:44 (UT) on December 17, 2008. Horizontal (longitude: ϕ) and vertical (latitude: λ) axes are expressed in polar coordinates. Point of $\phi = 180°$ and $\lambda = 0°$ indicates anti-sunward direction. (b): Model distribution of Na emission reproduced from Na emissions seen from different orbital positions of spacecraft during 14:01–14:44 (UT). (c–e): Model distributions of Na emission seen from spacecraft positions at 14:01, 14:19 and 14:41 (UT). (i–iii): Field-of-view of the spacecraft position at 14:01, 14:19 and 14:41 (UT), respectively.

of the orbiter and revolution period were ∼100 km and ∼90 min, respectively. Figure 1 shows the spacecraft orbit in the Moon-centered, solar ecliptic (MSE) coordinates on December 17, 2008. The black dotted line shows the spacecraft orbit, and the black and blue arrows indicate the normal of the orbital plane and the anti-sunward direction, respectively. The red arrows are the field-of-view directions at spacecraft positions during 14:01–14:44 (UT). The TVIS and TEX are mounted on a two-axis gimbal, with one axis (azimuth axis) normal to the orbital plane and the other (elevation axis) perpendicular to the azimuth axis. During our observation, the azimuth angle was fixed. Therefore, the field-of-view coverage of the sky was a sector strip with an angular width of 2.4° during a revolution of the spacecraft, as shown in Fig. 1. The elevation angle was moved by ∼3° in a 3-day period so that the anti-sunward direction was always included in the sector strip, which was made up of continuous images.

The position of the filter turret was changed at every observation revolution in the order of NaD, OI, and the shutter. The observing frames were taken at 65-s intervals with an exposure time of 30 s. Observations were made only when the spacecraft was in the shadow region of the Moon due to the capability of the Peltier cooler of the CCD sensor.

Although the spacecraft made 18 revolutions during the 9 days in which the observations of Na emission were made, due to a problem with CCD cooling, several datasets contain high dark noise. In this paper, we therefore present four datasets taken during the period, 17–19 December, 2008. The Moon stayed outside the magnetosphere dur-

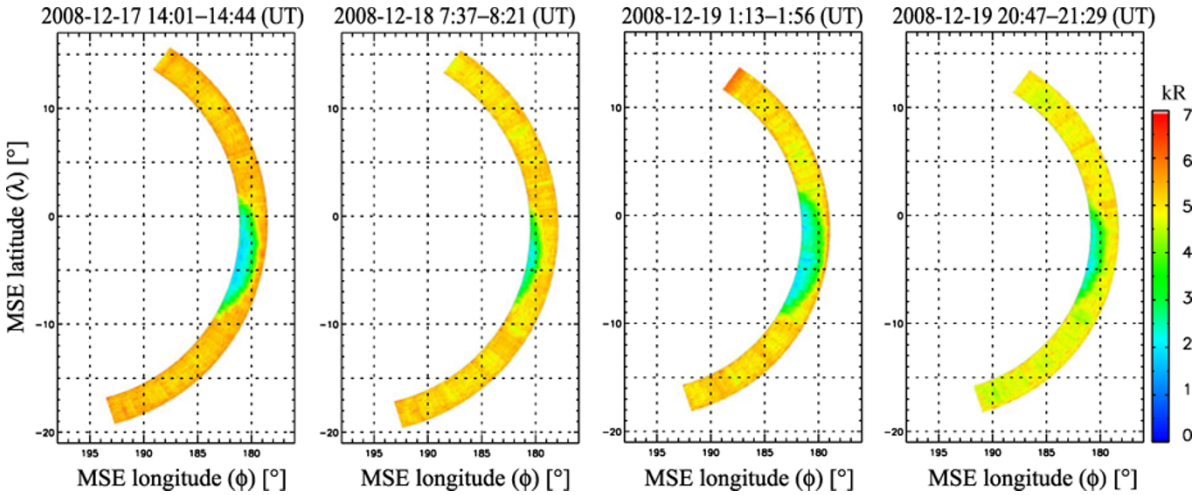

Fig. 3. Distributions of Na emission in MSE coordinates taken in four revolutions during the period 17–19 December, 2008.

ing the whole of the observation period. The observation parameters are summarized in Table 2.

3. Data Reduction

Data reduction was carried out as follows. First, the dark current was subtracted from the NaD and OI frames using shutter frames that were taken at almost the same orbital position, i.e., only a few revolutions before or after the NaD or OI frames were taken. Due to an electronic problem, the DC-offset level of the CCD signal varied from frame to frame. Therefore, careful determination of the DC-offset level for each frame was needed for the UPI-TVIS datasets. Because there was some overlap between continuing frames, we adjusted the DC-offset levels so that the median values in the overlap region became the same. Flat-fielding reduction and absolute intensity calibration steps were then carried out for the NaD and OI frames, using a laboratory calibration dataset (Taguchi *et al.*, 2009). Signals from the NaD frames can contain the background continuum as well as the lunar Na emissions. The intensities of the background continuum integrated within the bandwidth of the OI filter were less than 0.5 kR/2.0 nm for all of the OI frames, and these were subtracted from the NaD frames, assuming the same continuum intensities for both the NaD and OI frames.

4. Results

Figure 2(a) shows the distributions of the Na emissions in the Moon-centered, solar ecliptic (MSE) coordinates, produced by combining 39 frames, with overlaps acquired during 14:01–14:44 (UT) on December 17, 2008. The horizontal (ϕ) and vertical (λ) axes are expressed in polar coordinates. The point of $\phi = 180^\circ$ and $\lambda = 0^\circ$ indicates the anti-sunward direction. Note that Fig. 2(a) is not a distribution of Na emissions seen from a certain position in an orbit around the Moon; rather, it was made by combining frames taken at different positions of the spacecraft in different field-of-view directions. We can clearly see two regions in the distribution of Na emissions: one is a uniformly bright (5–6 kR) region and the other is a dark (2–3 kR) region. To identify these features, we attempted to reproduce the distribution of the Na emissions observed from orbital different positions of the spacecraft, as shown in Fig. 2(c–e). A spherically symmetric distribution of Na atoms expressed as below was used in the simulation,

$$n(z_{\rm gp}) = n_0 \exp\left(-z_{\rm gp}/H^*\right), \qquad (1)$$

where $z_{\rm gp} = R_{\rm m} z/(R_{\rm m} + z)$ is the geopotential height, $H^* = 300$ km is the apparent scale height, and $n_0 = 11$ cm^{-3} is the surface number density of the Na atoms (Sprague *et al.*, 1992). The model distribution of Na emission intensity was derived by integrating the number density of Na atoms along the line-of-sight within a distance smaller than 500 Moon radii, including the effects of the umbra and penumbra of the Moon. The efficiency of resonant scattering, the so called g-factor, was calculated by assuming that all of the atoms have no motion relative to the Sun. We can clearly identify two regions in the model distribution of Na emission shown in Fig. 2(c–e); one is a bright region (>5 kR) and the other is a dark one (<2 kR). The dark region corresponds to the shadow of the Moon because resonant scattering of Na atoms by solar radiation does not take place in the umbra of the Moon. The square regions in the model distribution, (i–iii), indicate the field-of-view of the TVIS at each position of the spacecraft. A sector strip of Na emission was then produced, as shown in Fig. 2(b), by combining the model distributions calculated at all orbital positions that correspond to different field-of-view directions. The observed emission intensity in the uniformly bright region in Fig. 2(a) is well reproduced by the model distribution in Fig. 2(b), although the observed brightness in the dark region, 2–3 kR, was much greater than that in the model distribution, 1–2 kR. As clearly shown by Wilson *et al.* (1999), the acceleration of Na atoms by solar radiation pressure results in a long-tail structure of Na atoms extending further than the distance between the Earth and Moon in an anti-sunward direction. Thus, the excess brightness in the dark region in the observation is presumed to be an emission from the Na tail region far beyond the umbra.

Figure 3 shows the changes in Na emission in the MSE coordinates taken during four revolutions in the period 17–19 December, 2008. The observed sector regions in the rev-

olutions are different because the spacecraft's orbital plane in the MSE coordinates moved toward the duskward ($-\phi$), and the elevation angle of the gimbal was moved 2° in the period 18–19 December so that the anti-sunward direction was kept in the field-of-view coverage. The emission intensity of the uniformly bright region gradually decreased during the 3-day period. The brightness of the dark region seemed to stay flat or to increase a little, although the observed coverage of the dark region was not sufficient to precisely determine the brightness.

5. Discussion

Figure 4(a) represents the variability in Na emission in the uniformly bright region shown in Fig. 3. During the 3-day period, the brightness decreased from 5.7±0.2 to 5.0±0.2 kR, which is 12±6%. Possible source mechanisms that could change the quantity of Na atoms emitted from the surface over several days include photodesorption, sputtering by solar wind particles, and micrometeorid impact. Below, we discuss which of these source mechanisms was responsible for the observed variability in Na emission.

High UV fluxes are supposed to increase the rate of photodesorption from the lunar surface. Figure 4(b) shows the variability in the $F_{10.7}$ index as a parameter of solar activity. The absolute values of $F_{10.7}$ in this period correspond to the solar minimum, and no particular changes can be seen. In addition, we did not see any significant variation in the X-ray flux monitor (CELIAS/SEM) onboard the SOHO spacecraft. Therefore, it seems unlikely that declining solar UV flux caused the declining Na exosphere that was observed.

Variability of the solar wind is the most plausible explanation for the changes observed in the Na exosphere. Figure 4(c) shows the variability of the proton flux observed by the WIND spacecraft, which was located upstream of the Earth. The thin solid line shows 1-h averaged values, and the thick solid line is the variation averaged during the previous 30 h. The decreasing tendency of the 30-h averaged proton flux appears to correspond well to the decay in Na. Approximately 1 day before our observation period, December 17–19, significant enhancement of the proton flux occurred on December 16, which was associated with a corotation interaction region. Delayed reactions in the Na exosphere, which reached up to 15 h after bombardment by the Earth's plasma sheet, were also reported by Wilson *et al.* (2006). As suggested by McGrath *et al.* (1986) for Mercury's Na exosphere, or by Potter *et al.* (2000), supposing that solar wind particles play a role in diffusing Na atoms or ions up to the surface, followed by Na atom ejection by photodesorption, the observed time lag seems to indicate the diffusion time scale.

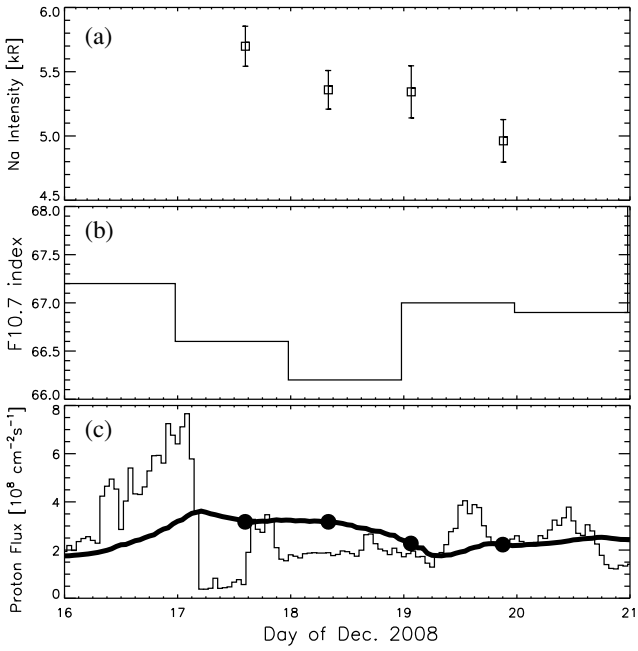

Fig. 4. (a): Variability in Na emission in uniformly bright region shown in Fig. 2. (b): Variation in $F_{10.7}$ index. (c): Variability of solar proton flux observed by WIND spacecraft. The thin solid line histograms indicate the 1-h averaged proton flux. The thick line indicates averaged proton flux variation for the previous 30 h. Filled circles are values observed at the times corresponding to 14:30, 8:00, 1:30, and 21:00 (UT) on 17, 18, 19, and 19 December, 2008, respectively.

Variability in micrometeoroid vaporization could also be a possible cause of the observed exospheric change. Leonid meteor showers are reported to increase the Na exosphere (Smith *et al.*, 1999; Wilson *et al.*, 1999) or to increase the scale height (Hunten, 1991; Hunten *et al.*, 1998; Verani *et al.*, 1998), although no enhancement was detected for Quadrantid meteoroids (Verani *et al.*, 2001). The Geminid meteor shower was active between December 7 and 17, reaching a maximum on December 13. Based on a report by the IMO Video Monitor network database, the number of meteors decreased by 20% on December 16, 2008, relative to the peak on 13–14 December, and then to less than a few percent of the peak on 17 December, although the Na exosphere was decreasing monotonously during the period 17–19 December. However, visible meteor rates do not necessarily correspond to meteoroid mass fluxes (Hunten *et al.*, 1991). Moreover, as pointed out by Verani *et al.* (2001), the mass flux of the Geminid meteor shower is the second-most intense meteor stream. Considering these facts, the decay in Geminid activity cannot be ruled out as a possible cause of the reduction in Na vaporization from the surface.

6. Conclusion

Resonant scattering emission from the Moon's sodium exosphere was detected from a lunar orbiter. The emission intensity decreased by 12±6% during a 3-day period, preceded by about 1 day by an enhancement of the solar proton flux. This result suggests that solar wind particles foster the diffusion of Na atoms or ions in the lunar regolith up to the surface and that the time scale of diffusion is around a few tens of hours. The decline in the activity of the Geminid meteor shower over this period is also a possible cause for the observed decay in the Na exosphere.

Acknowledgments. We thank Cesare Barbieri and an anonymous referee for their helpful comments and advice, all of which improved this paper. The authors would like to acknowledge all members of the SELENE mission team for their support of the operation.

References

Hodges, R. R., Jr., Helium and hydrogen in the lunar atmosphere, *J. Geo-*

phys. Res., **78**(34), 8055–8064, 1973.
Hodges, R. R., Jr., Formation of the lunar atmosphere, *Moon*, **14**, 139–157, 1975.
Hoffman, J. H., R. R. Hodges Jr., and D. E. Evans, Lunar atmospheric composition results from Apollo 17, *Proc. Lunar Sci. Conf., 4th*, 2875–2875, 1973.
Hunten, D. M., R. W. H. Kozlowski, and A. L. Sprague, A possible meteor shower on the Moon, *Geophys. Res. Lett.*, **18**, 2101–2104, 1991.
Hunten, D. M., G. Cremonese, A. L. Sprague, R. E. Hill, S. Verani, and R. W. H. Kozlowski, The Leonid meteor shower and the lunar sodium atmosphere, *Icarus*, **136**, 298–303, 1998.
Kato, M., S. Sasaki, K. Tanaka, Y. Iijima, and Y. Takizawa, The Japanese lunar mission SELENE: Science goals and present status, *Adv. Space Res.*, **42**, 294–300, 2008.
McGrath, M. A., R. E. Johnson, and L. J. Lanzerotti, Sputtering of sodium on the planet Mercury, *Nature*, **323**, 694–696, 1986.
Mendillo, M., J. Baumgardner, and J. K. Wilson, Observational test for the solar wind origin of the Moon's sodium atmosphere, *Icarus*, **137**, 13–23, 1999.
Potter, A. E. and T. H. Morgan, Discovery of sodium and potassium vapor in the atmosphere of the Moon, *Science*, **241**, 675–680, 1988.
Potter, A. E. and T. H. Morgan, Observations of the lunar sodium exosphere, *Geophys. Res. Lett.*, **18**(11), 2089–2092, 1991.
Potter, A. E. and T. H. Morgan, Variation of lunar sodium emission intensity with phase angle, *Geophys. Res. Lett.*, **21**(21), 2263–2266, 1994.
Potter, A. E., R. M. Killen, and T. H. Morgan, Variation of lunar sodium during passage of the Moon through Earth's magnetotail, *J. Geophys. Res.*, **105**, 15,073–15,084, 2000.
Smith, S. M., J. K. Wilson, J. Baumgardner, and M. Mendillo, Discovery of the distant lunar sodium tail and its enhancement following the Leonid meteor shower of 1998, *Geophys. Res. Lett.*, **26**, 1649–1652, 1999.
Sprague, A. L., R. W. H. Kozlowski, D. M. Hunten, W. K. Wells, and F. A. Grosse, The sodium and potassium atmosphere of the Moon and its interaction with the surface, *Icarus*, **96**, 27–42, 1992.
Stern, S. A., The lunar atmosphere: History, status, current problems, and context, *Rev. Geophys.*, **37**, 453–491, 1999.
Taguchi, M., T. Sakanoi, S. Okano, M. Kagitani, M. Kikuchi, M. Ejiri, I. Yoshikawa, A. Yamazaki, G. Murakami, K. Yoshioka, S. Kameda, F. Ezawa, T. Toyota, W. Miyake, M. Nakamura, and K. Shiokawa, The Upper atmosphere and Plasma Imager/the Telescope of Visible light (UPI/TVIS) onboard the Kaguya spacecraft, *Earth Planets Space*, 2009 (submitted).
Tyler, A. L., R. W. H. Kozlowski, and D. M. Hunten, Observations of sodium in the tenuous lunar atmosphere, *Geophys. Res. Lett.*, **15**(10), 1141–1144, 1988.
Verani, S., C. Barbieri, C. R. Benn, and G. Cremonese, Possible detection of meteor stream effects on the lunar sodium atmosphere, *Planet. Space Sci.*, **46**, 1003–1006, 1998.
Verani, S., C. Barbieri, C. R. Benn, G. Cremonese, and M. Mendillo, Possible detection of meteor stream effects on the lunar sodium atmosphere, *Mon. Not. R. Astron. Soc.*, **327**, 244–248, 2001.
Wilson, J. K., S. M. Smith, J. Baumgardner, and M. Mendillo, Modeling an enhancement of the lunar sodium atmosphere and tail during the Leonid meteor shower of 1998, *Geophys. Res. Lett.*, **26**, 1645–1648, 1999.
Wilson, J. K., M. Mendillo, and H. E. Spence, Magnetospheric influence on the Moon's exosphere, *J. Geophys. Res.*, **111**, A07207, doi:10.1029/2005JA011364, 2006.
Yamazaki, A., S. Tashiro, Y. Nakasaka, I. Yoshikawa, W. Miyake, and M. Nakamura, Sounding-rocket observation of O II 83.4-nm emission over the polar ionosphere, *Geophys. Res. Lett.*, **29**, 2005, 2002.
Yoshikawa, I., M. Nakamura, M. Hirahara, Y. Takizawa, K. Yamashita, H. Kunieda, T. Yamazaki, K. Misaki, and A. Yamaguchi, Observation of He II emission from the plasmasphere by a newly developed EUV telescope on board sounding rocket S-520-19, *J. Geophys. Res.*, **109**, 19897, 1997.
Yoshikawa, I., A. Yamazaki, G. Murakami, K. Yoshioka, S. Kameda, F. Ezawa, T. Toyota, W. Miyake, M. Taguchi, M. Kikuchi, and M. Nakamura, Telescope of extreme ultraviolet (TEX) onboard SELENE: science from the Moon, *Earth Planets Space*, **60**, 407–416, 2008.

M. Kagitani (e-mail: kagi@pparc.geophys.tohoku.ac.jp), M. Taguchi, A. Yamazaki, I. Yoshikawa, G. Murakami, K. Yoshioka, S. Kameda, F. Ezawa, T. Toyota, and S. Okano